Characterization of Oscillatory Boundary Layer over a Closely Packed Bed of Sediment Particles

Chaitanya D. Ghodke, Joseph Skitka and Sourabh V. Apte

Reprinted from

The Journal of
Computational Multiphase Flows

Volume 6 · Number 4 · 2014

Multi-Science Publishing

Characterization of Oscillatory Boundary Layer over a Closely Packed Bed of Sediment Particles

Chaitanya D. Ghodke*, Joseph Skitka and Sourabh V. Apte
School of Mechanical, Industrial, and Manufacturing Engineering,
Oregon State University, USA

Received: 15 July 2014; Accepted: 1 September 2014

Abstract

Lack of accurate criteria for onset of incipient motion and sediment pickup function remain two of the biggest hurdles in developing better predictive models for sediment transport. To study pickup and transport of sediment, it is necessary to have a detailed knowledge of the small amplitude oscillatory flow over the sediment layer near the sea bed. Fully resolved direct numerical simulations are performed using fictitious domain approach (Apte & Finn, 2012) to investigate the effect of a sinusoidally oscillating flow field over a rough wall made of regular hexagonal pack of spherical particles. The flow arrangement is similar to the experimental data of Keiller & Sleath (1976). Transitional and turbulent flows at Re_δ = 95, 150, 200 (based on the Stokes layer thickness, $\delta = \sqrt{2\nu/\omega}$) are studied. Turbulent flow is characterized in terms of coherent vortex structures, Reynolds stress variation and PDF distributions. The nature of unsteady hydrodynamic lift forces on sediment grains and their correlation to sweep and burst events is also reported. The dynamics of the oscillatory flow over the sediment bed is used to understand the mechanism of sediment pick-up.

1. INTRODUCTION

A river or sea bed is made up of sediment particles that are in close contact with each other and retain the form of the bed through collision and cohesive forces (Fredsoe & Deigaard 1992). Shear stress due to fluid flow can mobilize and transport these particles as bed-load (partially mobile bed of dense particles). Stresses exceeding a critical threshold can strip the particles from the bed, suspend them in the fluid and deposit them elsewhere.

Prediction of onset of sediment erosion and interactions of sediment bed with oscillatory turbulent flows are the two long-standing issues governing sediment transport in coastal environments. Computations of sediment-laden flows typically employ simplistic models (Fredsoe & Deigaard, 1992, Nelson 2000) for (i) incipient motion and resultant bed-load transport, and (ii) suspended sediment transport. Historically, quasi-steady models used to predict incipient motion in steady as well as oscillatory coastal environments, are based on the *Shield's parameter* (Nelson *et al*. 2000, Bagnold 1966, Nino *et al*. 2003), which is the ratio of average bed shear stress to the stabilizing settling force due to gravitational acceleration. The mean bed-load particle flux is then obtained as a function of particle size and bed shear stress. Sleath and co-workers (Sleath 1995, Flores & Sleath 1998) identified that in wave-induced sediment transport, pressure-gradient at the peak of the cycle should be accounted for and defined the *Sleath's parameter* for onset of erosion. Laboratory observations have tried to quantify onset of erosion based on exceeding the Shield's or Sleath's parameters beyond a critical value. Using field studies, Foster *et al*. (2006) argued that combination of the bed shear stress and the maximum pressure gradient, that is, both Shield's and Sleath's parameters are important for onset of erosion.

It is well known that in wall-bounded, single-phase turbulent flows, the near wall structures are arranged in alternating high and low-speed streaks of momentum regions that evolve into characteristic vortical structures (Moin & Mahesh 1998), *sweeps* (injection of high-speed fluid toward the wall), and *bursts* (low-speed ejections from the wall) are the major contributors to the Reynolds stress, whereas bursts are responsible for the turbulent energy production and

* Corresponding author: E-mail: ghodkec@onid.orst.edu

transport mechanisms. Drake and co-workers (Drake & Calantoni 2001, Nelson *et al*. 1995) have used motion-picture photography to observe bed-load transport and effects of the sweep-burst cycles on entrainment (rolling, liftoff, ejection), displacement (saltation, rolling, sliding), distrainment (or cessation of displacement), and repose. In the presence of particles, these sweep-burst cycles directly influence the particle entrainment and deposition. Bursts are effective in entraining particles in low-speed, low-vorticity, and high-strain regions (Kaftori 1995a, Kaftori 1995b). Experimental data and Discrete Element Model predictions for accelerating flows over river bed forms (Schmeeckle & Nelson 2003, Schmeeckle *et al*. 2007) and oscillatory flows in coastal environments (Calantoni & Drake 1998, Drake & Calantoni 2001) support the hypothesis that sediment-transport models cannot be based on average boundary shear-stress alone. Flow parameterizations and predictive models accounting for the multi-scale interactions among the bed shear-stress, near-wall turbulence, and particle dynamics are needed.

As the first step towards fundamental understanding of sediment incipient motion in coastal environments, a detailed fully resolved simulation (FRS) of oscillatory boundary layers over a closely stacked sediment particles is performed at various Reynolds numbers wherein the sediment particles are held fixed. The goal is to quantify the nature of the unsteady forces (lift) on the particles and their correlations with the oscillatory turbulent flow characteristics such as near-wall structures, Reynolds stress, local acceleration, amongst others. The oscillatory flow is modeled as a small amplitude monochromatic wave generated by a sinusoidally oscillating pressure gradient. In this configuration, a single layer of sediment particles are arranged in hexagonal close-pack similar to the experimental work by Keiller and Sleath (1976). In this work, this experimental configuration is used as an initial test case to investigate the effect of vortex structures shed by the sediment particles on the bed shear stress and the lift and drag forces.

Fully resolved simulations have only become possible recently owing to advancement in numerical algorithms and computational infrastructure. There has been considerable work done on steady flows in open channels over fully resolved spherical sediment elements which can be ejected and entrained in the flow (Chan-Braun *et al*. 2011). Recently, FRS was used to study flow over roughness elements in oscillatory flows corresponding to the experimental work by Keiller and Sleath (1975) [referred to as K&S] by Fornarelli and Vittori (2009) [referred to as F&V] using immersed boundary method, Ding & Zhang (2010) [referred to as D&Z] using the Lattice Boltzmann method. However, both of these studies involved sediment particles that were not in direct contact with each other but had a small gap in between in a hexagonal packing arrangement. F&V used semi spheres rather than full particle and it is hypothesized that full spheres in direct contact with each other will have different flow features than the ones studied by them. Thus, in this work, a hexagonally packed layer of particles that are in contact with each other are simulated in an oscillatory boundary layer and compared with the experimental data.

The overall structure of this article is as follows: In section 2, the information about computational setup and flow conditions is presented. Section 3 presents details of numerical methodology used in this study. Section 4 contains results of all simulations in terms of grid refinement study, validation study, turbulent flow characteristics followed by force field analysis. Section 5 presents concluding remarks along with future scope of work.

2. COMPUTATIONAL SETUP

Figure 1 shows the computational domain and hexagonally packed particle orientation used in the present study. The computational domain consists of a doubly periodic box (x and y co-ordinates) with a smooth wall at z = 0 and a slip wall at z = 30δ, where $\delta = \sqrt{2\nu/\omega}$ is the Stokes layer thickness, ν is the kinematic viscosity, and ω is the oscillation frequency. The domain is 24.076δ long in the flow direction and 13.9δ wide in the span-wise direction both of which are assumed periodic. The non-dimensional sediment particle diameter is d = D/δ = 6.95, giving roughly 13 sediment particles in the domain. The computational domain size is chosen similar to the previous computational work by Fornarelli and Vittori (2009), although larger domains would be more favourable to obtain better statistic; these will be utilized in the near future of this project. Reynolds numbers can now be defined based on the free-stream maximum velocity U_0, Stokes layer thickness (δ), the particle diameter (D), or the oscillation amplitude (*A*) as,

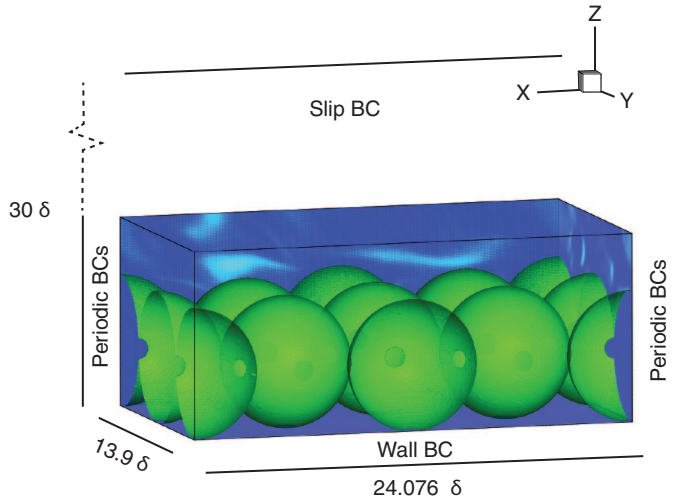

Figure 1: Schematic of the computational domain and boundary conditions. The flow field is setup by imposing sinusoidal pressure forcing that gives rise to the flow velocity far from the wall as $(u,v,w) = (U_0\sin(\omega t),0,0)$, where U_0 is the amplitude of fluid velocity oscillation.

$$Re_\delta = \delta U_0 / \nu = 95 \leq Re \leq 200 \tag{1}$$

$$Re_D = DU_0 / \nu = 660 \leq Re \leq 1390 \tag{2}$$

$$Re_A = AU_0 / \nu = U_0^2 / \omega\nu = Re_\delta^2 / 2 = 4500 \leq Re \leq 20000 \tag{3}$$

The range of Reynolds numbers investigated is given in the above expressions. The Reynolds number and the non-dimensional particle diameter uniquely define the two degrees of freedom of this flow.

3. NUMERICAL SCHEME

The numerical approach for the fully resolved simulations is based on a fictitious domain method (FDM) wherein the grid region occupied by the particles is treated as a fluid of density equal to the particle density (relevant only for freely moving particles) and the Navier-Stokes equations together with the incompressibility constraint are solved over the entire domain. The flowfield inside the particle region is constrained to undergo rigid body motion (translational and rotational) by a rigidity constraint force that is non-zero only within the particle region. A novel algorithm that facilitates solution of freely moving particles for a wide range of fluid-particle density ratios was developed (Apte & Finn, 2012) and is used in the present work. The details of the algorithm as well as very detailed verification and validation studies have been published elsewhere and here only a summary of the basic algorithm is presented.

The governing equations are solved using a three-level fractional-time-stepping method. First, the momentum equations without the rigidity constraint force are solved, using symmetric energy conserving discretization (Apte & Finn, 2012) over the entire domain. The incompressibility constraint is then imposed by setting up a pressure Poisson equation (obtained by taking the divergence of the momentum equation). The resultant velocity field satisfies the incompressibility constraint but may not provide the necessary rigid body motion within the particle region. The velocity field within the particle domain can be decomposed into a rigid body component ($\mathbf{u}^{RBM}$) and the deformation component ($\mathbf{u'}$). For the present study, the sediment particles are held fixed, and hence the rigid body motion is completely known a priori ($\mathbf{u}^{RBM} = 0$). The rigidity constraint force is then simply obtained as, $\mathbf{F}_R = -\rho_p\, u'/\Delta t$, where ρ_p is the particle density, Δt is the time step

used and u' is the non-zero velocity field within the particle region obtained from the solution of the incompressible Navier-Stokes equations. The solver based on this fictitious domain method is fully parallel and uses non-uniform Cartesian grids. A detailed verification and validation study has been performed (Apte & Finn, 2012).

4. RESULTS AND DISCUSSION

The numerical approach is first used to identify the grid resolution required to obtain accurate results by performing a grid-refinement study on a shorter domain with fewer particles. A thorough analysis looking at the energy spectra with grid refinement was used to assess the grid resolution requirement. The solver was then used to perform FRS studies at different Reynolds numbers and results were compared with the available experimental data to show good agreement. The numerical data was also analysed in detail to study the effect of the oscillatory flow and sediment-bed interactions on the forces on the particles.

4.1 Grid-refinement study

In order to obtain details on the grid resolution requirement needed for the simulations involving turbulent flow over closely packed sediment particles, a detailed grid refinement study with only one layer of particles and in a shorter domain than that shown in Fig. 1 was performed. Using a very fine resolution as the ideal solution, the maximum error in the axial velocity field obtained in these studies versus the grid resolution is plotted in Fig. 2 to show a nearly second-order convergence. This confirms that the overall accuracy of the solver is second-order. In addition, to obtain the temporal variations of the velocity and other flow parameters, energy spectra were analysed for different grid resolutions keeping the Courant number (CFL) close to 0.5 for time-accurate calculations. The convergence of energy spectra with grid resolution provided insights into the necessary resolution for these calculations.

It was found that in the sediment particle region, close to 100 grid points per particle diameter are needed to obtain good spatial-temporal data. In order to maintain good accuracy, stretched grids are not preferred with the present numerical scheme, however, grid elements need not be cubic. Accordingly, use of 50 grid points per particle diameter in the periodic x-direction (stream-wise) and 100 per particle diameter in the flow normal z-direction and periodic y-direction (span-wise) was found to provide similar accuracy as a fully uniform cubic grid. In order to keep the grid size small, the uniform grids are used only in the region surrounding the particles, and the grids are stretched in the flow normal direction using hyperbolic tangent function typically used in boundary layer and channel flow calculations (Moin & Mahesh, 1998). Table 1 provides the grid resolutions used for three different Reynolds number studied in this work.

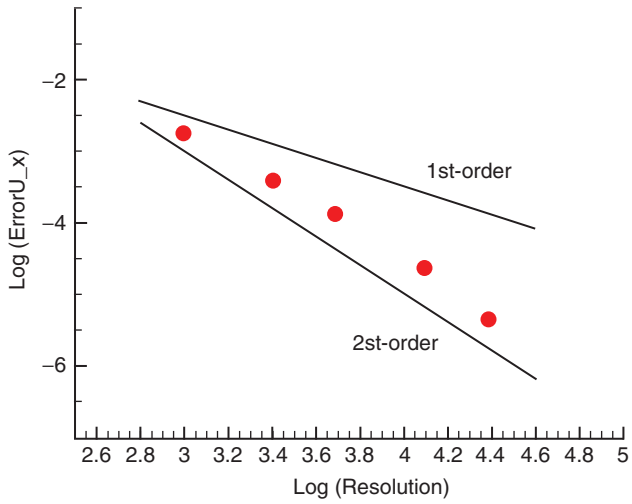

Figure 2: Grid convergence study showing max error in axial velocity as a function of the grid resolution. Second-order accuracy is observed.

Table 1. Grid resolution for different Reynolds numbers used in the study

Re_d	Re_D	Re_A	N_x	N_y	N_z
95	660	4500	136	160	232
150	1042	11250	172	200	292
200	1390	20000	208	240	344

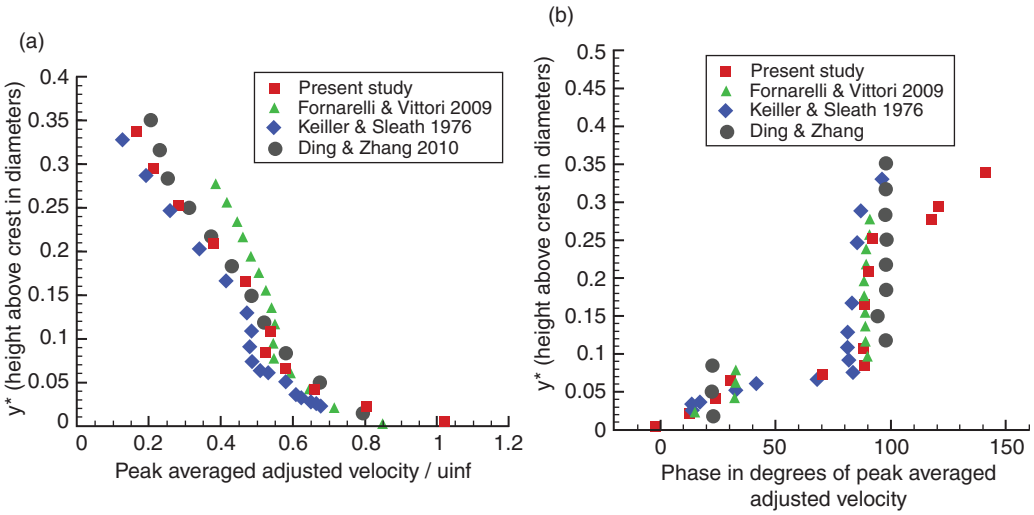

Figure 3: Variation of normalized peak fluid-frame velocity magnitude (a, left) and phase (b, right) with respect to the height at crest ($Re_\delta = 95$) compared with the experimental and other simulation data.

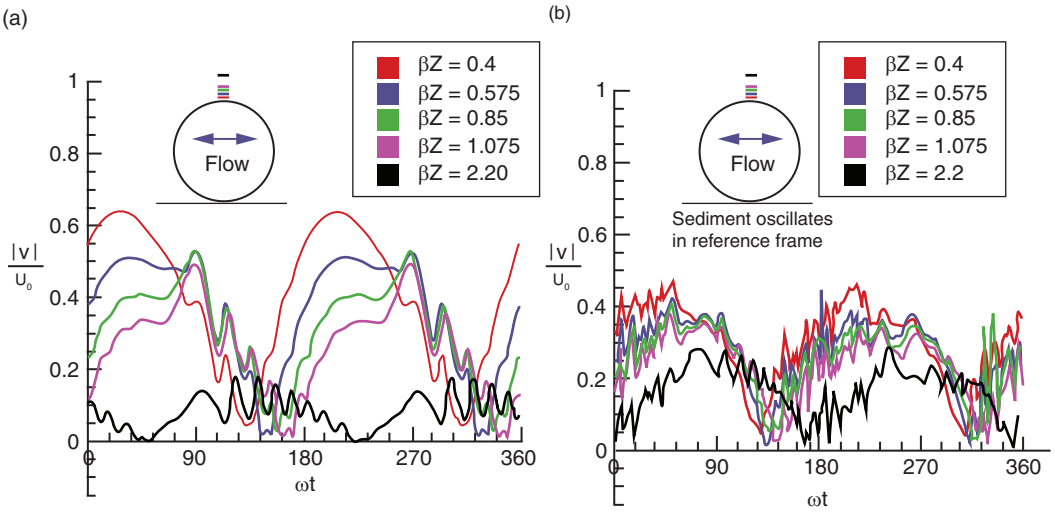

Figure 4: Variation of normalized fluid-frame velocity over a cycle at different heights above the crest of the particle: (a) $Re_\delta = 95$, (b) $Re_\delta = 200$. Here, $\beta = 1/\delta$.

4.2 Validation study

In order to validate the computational predictions, the numerical data for $Re_\delta = 95$ is first compared with the experimental data of K&S (1976) as well as computations by F&V and D&Z. Existing literature pertaining to this topic frequently uses an alternative frame of reference, consistent with that of the classic experiments conducted K&S, which feature an oscillating sediment bed in a fixed fluid frame (the surrounding air). Figures 3 and 4 are presented in the fluid frame to be consistent with this convention.

Figure 3a depicts the variation of the peak phase-averaged velocity (in the oscillating fluid frame) with respect to the height above the sediment crest. The velocities are localized above the crests. Data from the present study is plotted along with recent simulations of D&Z and F&V, as well as the experimental data of K&S. This data is generally in a better agreement with the experimental than that of the other simulations, suggesting the present geometry (specifically the use of touching spheres and pore space), solver resolution, and rigid-body treatment used in the present fictitious domain method are able to provide accurate description of the oscillatory-flow phenomena. Figure 3b compares the phase at which the peak velocity is recorded and shows good agreement between K&S and the present study. Take a note that the vertical trends in both plots starting around $z/\delta = 0.1$ are artefacts of the ejection of coherent vortex structures at peak velocity.

Figure 4a shows averaged velocity as a function of phase at several points above the sphere crest for $Re_\delta = 95$. These can be compared with Fig. 4 in the experimental work of K&S. The plot should be approaching a sinusoidal profile in the limit as βz (normalized height with $\beta = 1/\delta$) approaches zero; the data of K&S features fluctuations in this limit crest ($\beta z<0.4$) which are not present in the simulations. This is attributed to perturbations inherently present in experiments. With the exception of this difference, the simulations capture the flow characteristics well; both show a secondary maximum in the fluid-frame velocity field occurring after the primary maximum during each cycle. K&S showed that the secondary peaks were due to strong vertical velocities causing momentum transport from high to low speed regions. The existence of horseshoe-type vortical structures was found in the present numerical studies. Figure 4b shows the same data for $Re_\delta = 200$. At increased Reynolds number, the velocity field closer to the sphere crest shows more perturbations that are sustained. In addition, the velocity field away from the sphere crests also show larger fluctuations owing to higher inertial effects. The simulation data yield a clarity of trends that is ideal for developing empirical models of flow properties and confirm that they are indeed able to reproduce the experimental observations accurately.

4.3 Turbulent flow structures

Interactions of sediment particles with the turbulent flow is a complex process and is greatly influenced by local flow structures present in the near wall region of turbulent flows. These flow structures are repeating and organized in nature and therefore are termed as "coherent flow structures". The effect of these structures on turbulent flow characteristics of the flow field can be analyzed by means of quadrant analysis which involves decomposition of Reynolds stress into four quadrants and are referred as outward interactions, ejections, inward interactions and sweeps; discussed in (Nelson 1995).

According to the present simulations, the flow experiences a transition to turbulence somewhere between $Re_\delta = 95$ and becomes fully turbulent at around $Re_\delta = 150$. The empirical relation adapted from Eq.5 of Sleath (1988) indicates that the flow is almost fully turbulent at $Re_\delta = 95$. It is possible that the transition is somewhat affected by the geometrical and resolution choices as well as the size of the domain used. In addition, the empirical relation derived based on experimental data may also not predict the transition region accurately owing to inherent perturbations present in the setup. This section presents turbulent flow analysis in terms of near-wall coherent flow structures and Reynolds stress variation for fully developed turbulent cases of $Re_\delta = 150$ and 200.

Figure 5 shows variation of normalized phase-averaged Reynolds stress (for $Re_\delta = 150$ and 200) at the crest of the particle for different phases in the flow cycle. As expected, Reynolds stress peaks close to the wall, both for $Re_\delta = 150$ and $Re_\delta = 200$ and then diffuses in the vertical direction for deceleration phases ($\omega t > 6\pi/10$). Compared to $Re_\delta = 150$, peak in the Reynolds stress for $Re_\delta = 200$ occurs much earlier in the flow cycle. This shows that for higher Reynolds numbers fully developed turbulence state occurs earlier and is present during most of the cycle of oscillation.

Following the approach by Jeong & Hussain (1995), coherent flow structures in the near wall region of the turbulent flow are identified using λ_2 parameter. Figure 6 shows iso-surface of λ_2 plotted at various phases in the flow cycle for $Re_\delta = 150$ and 200. As flow begins to accelerate, low speed streaks get elongated in the stream-wise direction (see Fig. 6[I-II]). Eventually these elongated streaks get uplifted as a result of strong ejection motions and form horseshoe vortices (see Fig. 6[III]). Later in the flow cycle, local flow instability then causes head of these horseshoe vortices to oscillate. Towards the end of deceleration phase these horseshoe vortices burst into the outer boundary layer by occurrence of sweep events (see Fig. 6[IV]). Compared to $Re_\delta = 150$, more of these near-wall flow structures are seen in the case of $Re_\delta = 200$. Also for $Re_\delta = 200$, occurrence

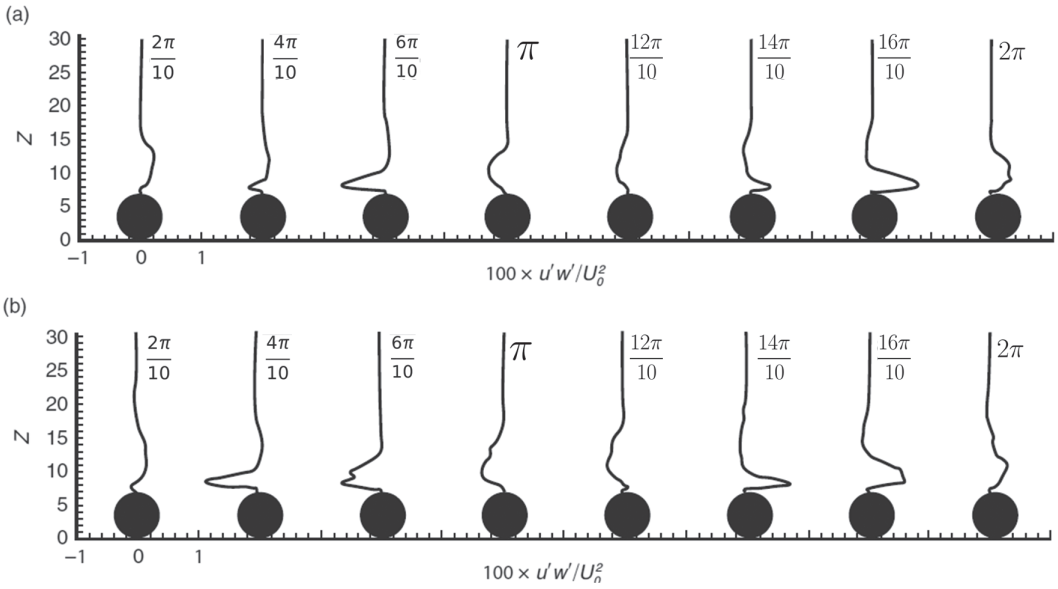

Figure 5: Variation of normalized phase-averaged Reynolds stress over a cycle plotted at the crest of the particle for: (a) Re_δ = 150, (b) Re_δ = 200.

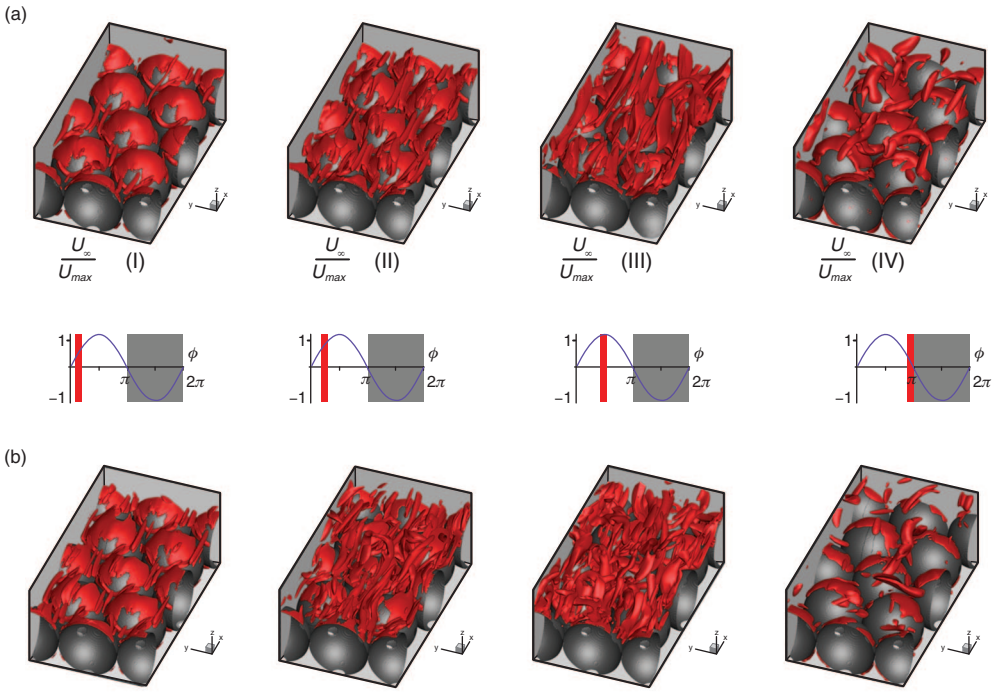

Figure 6: Iso-surface of $\lambda_2 = -0.02\frac{U_0^2}{\delta^2}$ at various phases for (a) Re_δ = 150 (b) Re_δ = 200.

of horseshoe vortices is seen much earlier in the flow cycle. This is in accordance with the earlier occurrence of peak Reynolds stress in the flow cycle for Re_δ = 200 (see Fig. 5b). The presence of these structures was speculated by Keiller & Sleath (1976), however, the experiments did not visualize such structures based on the data collected. The simulations are thus very informative and confirm the presence of these near-wall flow structures. As noted earlier, these sweep and ejection motions contribute positively towards the Reynolds stress and might play important role in

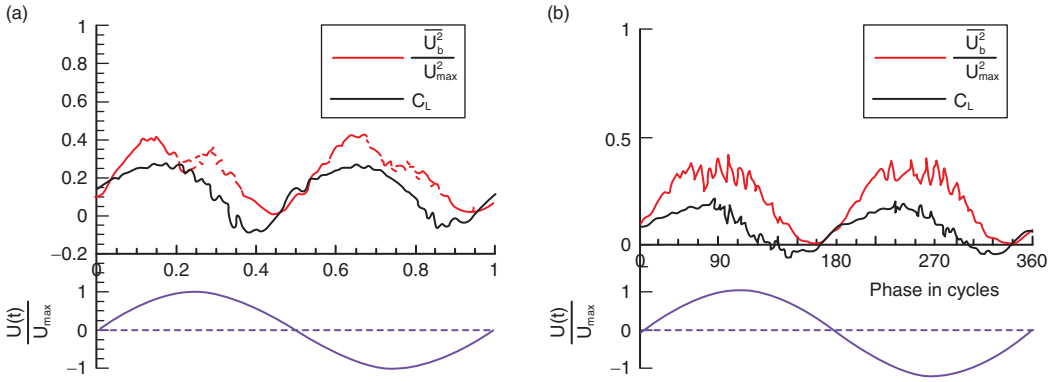

Figure 7: Distribution over a cycle of the lift coefficient and normalized U^2 averaged over the Stokes layer: (a) $Re_\delta = 150$, (b) $Re_\delta = 200$.

destabilizing the particle. It would, therefore, be important to study effect of these structures, if any, on hydrodynamic forces on particles.

4.4 Force field analysis

The aim of this investigation is to shed light on flow characteristics which may be used to improve existing sediment transport models for oscillatory flow. One promising avenue to approach this is to develop models for the probability distribution functions of the lift on a sediment element as a function of phase and other flow parameters. Experimentally, it is much easier to measure the velocity square as opposed to lift forces on individual sediment particles and it is natural to correlate it with the lift forces. Figures 7a and 7b plot the variation over a cycle of lift coefficient and non-dimensionalized velocity squared above the sediment element averaged over the Stokes layer for Re_δ=150 and 200, respectively. The lift coefficient values are in close agreement with the experimental data of Rosenthal and Sleath (1986). The net lift coefficient remains positive over the cycle and has a period of half the forcing function. Phase averaged lift force was found to be well correlated with the phase averaged squared velocity within the Stokes layer, although a small phase difference was observed. This is a critical result for development of models for lift forces based on the flow velocity near the sediment bed. For both Re_δ = 150 and 200, lift coefficient reaches maximum when the horseshoe vortex intensity reaches maximum. This further provides the evidence of the direct link between Reynolds stress, coherent flow structures and unsteady hydrodynamic forces on sediment particles.

In order to further explore the possibility of developing probabilistic models for sediment dislodgment, it would be of interest to analyze probability density functions (PDFs) of $U^{2'}$ in the flow cycle. Figure 8 and 9 show PDFs of non-dimensionalized velocity-squared fluctuations ($U^{2'}$) in the flow cycle for Re_δ = 150 and 200, respectively. The PDF distributions show non-Gaussian behavior away from the flow reversal phases (see Fig. 8-9 II-VIII) when ejection and sweep motions are dominant; substantiating the presence of link between near-wall structures and unsteady hydrodynamic forces on sediment particles. The peaked-ness of the PDFs as well as long positive tails may be critical for incipient motion modeling. Broad models of lift and flow characteristics in oscillatory flow will continue to be sought after as larger simulations over a more diverse set of parameters are executed.

5. CONCLUSIONS

In this work, fully resolved simulations of transitional and turbulent oscillatory flows over a fixed layer of hexagonally packed sediment bed corresponding to the experimental setup of Keiller & Sleath (1976) were performed. The flow field was driven by a periodic sinusoidal pressure variation. The predicted magnitudes and phases of averaged velocity were compared with the experimental data and also numerical studies by Fornarelli & Vittori (2009) and Ding & Zhang (2010). The present results showed better predictions compared to the experiments which may be

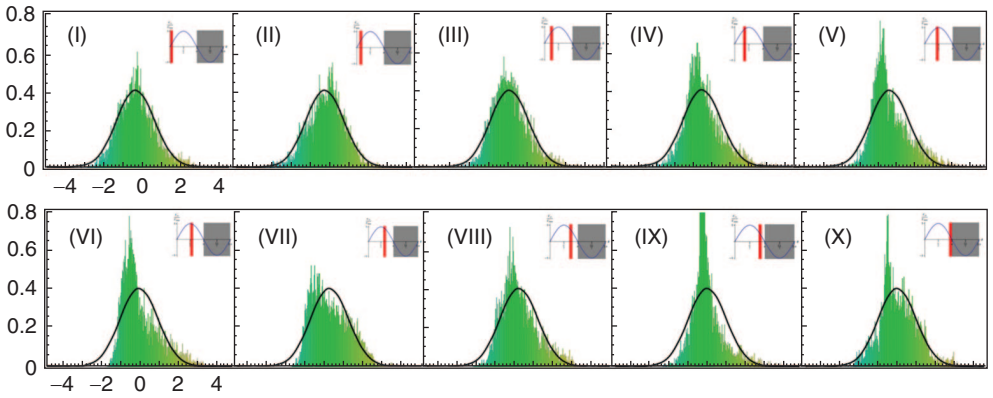

Figure 8: PDF of non-dimensionalized velocity-squared fluctuations $(U^2)'$ in the flow cycle for $Re_\delta = 150$.

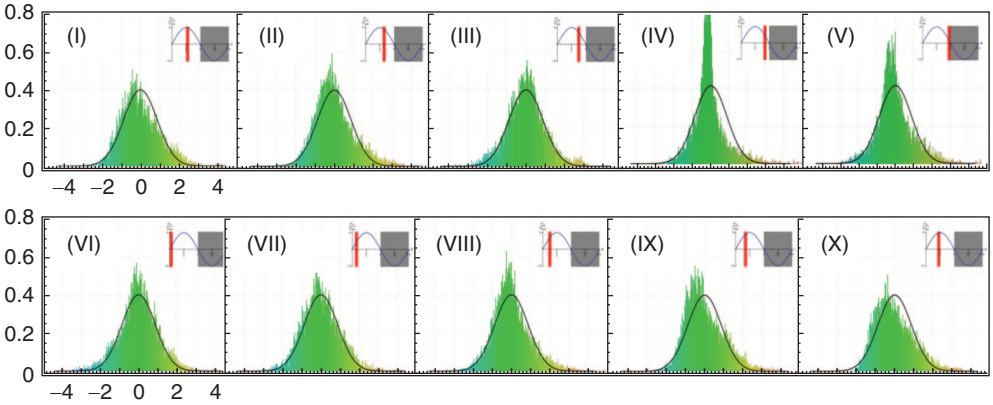

Figure 9: PDF of non-dimensionalized velocity-squared fluctuations $(U^2)'$ in the flow cycle for $Re_\delta = 200$.

attributed to the fact that the present work involved full spheres that were in close contact with each other, unlike the prior simulations.

The turbulent flow structures were analysed in detail to show presence of strong horseshoe vortices (as a consequence of ejection and sweep motions). Occurrence of these horseshoe vortices and the pressure minima on the top of the spheres lead to variations in the lift forces on the spheres. Lift coefficient reaches maximum when the horseshoe vortex intensity reaches maximum. There exists enough evidence of the direct link between Reynolds stress, coherent flow structures and unsteady hydrodynamic forces on sediment particles.

Two positive peaks were observed in the lift coefficient per cycle for the range of Re_δ studied. The phase averaged lift force was found to be well correlated with the phase averaged $u^{2'}$ within the Stokes layer, although a small phase difference was observed. The PDF distributions of the velocity fluctuations show non-Gaussian behaviour away from the flow reversal phases when ejection/sweep events are dominant. Large variations were observed at peak phases that may be critical for incipient motion. Additional computations varying the parameter range and larger domain sizes are necessary to obtain better statistics and are planned as part of the future work.

ACKNOWLEDGEMENTS

The work is funded by NSF-CBET project number #1133363. The computations were performed on Texas Advanced Computing Center's Lonestar machine.

REFERENCES

[1] Apte, SV & Finn, J., A variable-density fictitious domain method for particulate flows with broad range of particle-fluid density ratios, J. Comp. Physics, *accepted for publication*, 2012.

[2] Bagnold, R., An approach to the sediment transport problem from general physics, US Geological Survey Professional Paper, Vol. 422(1), 1–37, 1966.

[3] Calantoni, J. & Drake, T., Discrete-particle model for nearshore bedload transport, EOS Trans. AGU, Vol. 29(17), Spring Meeting, Suppl 112, 1998.

[4] Chan-Braun, C., Garcia-Villalba, M, & Uhlmann, M., Force and torque acting on particles in transitionally rough open-channel flow, Journal of Fluid Mechanics, Vol. 684, 441, 2011.

[5] Ding, L & Zhang, Q-H, Lattice-Boltzmann simulation to characterize roughness effects of oscillatory boundary layer flow over a rough bed, Coastal Engineering, 1–11, 2010.

[6] Drake, T., & Calantoni, J., Discrete particle model for sheet flow sediment transport in nearshore, Journal of Goephysical Research, Vol. 106(C9), 19859–19868, 2001.

[7] Fornarelli, F. & Vittori, G., European Journal of Mechanics B/Fluids, Vol. 28, 283–295, 2009.

[8] Foster, D., Bowen, A., Holman, R., & Natoo, P., Field evidence of pressure gradient induced incipient motion, Journal of Geophysical Research, Vol. 111(C05004), 2006.

[9] Fredsoe, J, & Deigaard, R., Mechanics of Coastal Sediment Transport, World Scientific, 1992.

[10] Jeong, J. & Hussain, F., On the identification of a vortex, J. Fluid Mech., Vol. 285, 67–94 (1995).

[11] Kaftori, D., Hetsroni, G., & Banerjee S., Particle behaviour in the turbulent boundary layer I., Motion, deposition, and entrainment, Physics of Fluids, Vol. 7(5), 1095–1106, 1995a.

[12] Kaftori, D., Hetsroni, G., & Banerjee S., Particle behaviour in the turbulent boundary layer II., Velocity and distribution profile, Physics of Fluids, Vol. 7(5), 1107–1121, 1995b.

[13] Keiller, D.C. & Sleath, JFA, Velocity measurements close to a rough plate oscillating in its own plane, J. Fluid Mech., Vol. 73, 673–691 (1976).

[14] Moin, P. & Mahesh, K., Direct numerical simulation: A tool in turbulence research, Annual Review of Fluid Mechanics, Vol. 30(1), 539–578, 1998.

[15] Nelson, J., Schmeeckle, M., Shreve, R. & McLean S., Sediment entrainment and transport in complex flows, Selected papers in International Association of Hydraulic Research Symposium on River, Coastal and Estuarian Morphodynamics, Genova, Italy, 2000.

[16] Nelson, J., Shreve, R., McLean S., & Drake, T., Role of near-bed turbulence structure in bed load transport and bed form mechanics, Water Resources Research, Vol. 31(8), 2071–2086, 1995.

[17] Nino,Y., Lopez, F. & Garcia M., Threshold for particle entrainment into suspension, Sedimentology, Vol. 50 (2), 247–263, 2003.

[18] Rosenthal, GN & Sleath, JFA, Measurements of lift in oscillatory flow, J. Fluid Mech., Vol. 164, 449–467, 1986.

[19] Schmeeckle, M., & Nelson J., Direct numerical simulation of bedload transport using a local, dynamic boundary condition, Sedimentology, Vol. 50(2), 279–301, 2003.

[20] Schmeeckle, M, Nelson, J., & Shreve, R., Forces on stationary particles in near-bed turbulent flows, Journal of Geophysical Research, Vol. 112(F02003), 2007.

[21] Singh, K. M., Sandham, N. D., and Williams, J. J. R. Numerical Simulation of Flow over a Rough Bed, Journal of Hydraulic Engineering, Vol 133, 386–398, 2007.

[22] Sleath, JFA, Sediment transport by waves and currents, Journal of Geophysical Research, Vol. 100(C6), 10977, 1995.

[23] Flores, N & Sleath JFA, Mobile layer in oscillatory sheet flow, Journal of Geophysical Research, Vol. 103(C6), 12783, 1998.

[24] Sleath, JFA, Turbulent oscillatory flow over rough beds, J. Fluid Mechanics, Vol. 182, 369–409, 1987.

[25] Sleath, JFA, Transition in Oscillatory Flow over Rough Beds, Journal of Waterway, Port, Coastal, and Ocean Engineering, Vol 114, No 1, 18–33 (1988).